



CDF/PUB/EXOTIC/PUBLIC/9586

## Search for a Fermiophobic Higgs Boson with the Diphoton Final State at CDF

The CDF Collaboration

*URL <http://www-cdf.fnal.gov>*

(Dated: October 30, 2008)

### Abstract

A search for the Higgs boson in the di-photon decay channel is reported. The Standard Model branching fraction is small, but other models - such as fermiophobic models where the Higgs does not couple to fermions - predict much larger branching fractions for the di-photon decay. Here a study is reported which used CDF data to place the strongest limit to date by a hadron collider on models of this type.

*Preliminary Results Winter 2008*

$m_{h_f}$ (GeV)	$\sigma(W_{associated})$ pb	$\sigma(Z_{associated})$ pb	$\sigma(VBF)pb$	$Br(h_f \rightarrow \gamma\gamma)$
70	0.88	0.47	0.18	0.81
80	0.60	0.32	0.15	0.70
90	0.42	0.23	0.13	0.41
100	0.30	0.17	0.11	0.18
110	0.22	0.12	0.09	0.062
120	0.16	0.093	0.08	0.028
130	0.12	0.071	0.06	0.019
140	0.09	0.055	0.06	0.0061
150	0.07	0.041	0.05	0.0020

TABLE I: Cross section for SM higgs production, and  $h \rightarrow \gamma\gamma$  branching fractions for the fermiophobic benchmark model.

## I. INTRODUCTION

Low mass Higgs boson searches at the Tevatron usually focus on the dominant  $b\bar{b}$  decay channel. The di-photon final state is appealing because the photon ID efficiency and energy resolution are much better than b-jets. Better energy resolution leads to a narrow  $M_{\gamma\gamma}$  mass peak which can be exploited to reduce background. However, in the standard model the branching fraction for the di-photon ( $\gamma\gamma$ ) final state,  $Br(h \rightarrow \gamma\gamma)$ , has a maximal value of approximately 0.2 % for Higgs boson masses of about  $120 GeV/c^2$  and this fact renders a discovery in this channel impossible.

In addition to standard model  $h \rightarrow \gamma\gamma$  production, one can devise many possible beyond standard model scenarios where the  $Br(h \rightarrow \gamma\gamma)$  is enhanced [1]. Here, the consequences of a so-called “fermiophobic” model where the Higgs boson has suppressed couplings to fermions will be studied. The fermiophobic Higgs ( $h_f$ ) benchmark model considered here assumes standard model coupling to bosons and vanishing couplings to all fermions. For such a model, the branching fractions for  $h \rightarrow \gamma\gamma$  is significant for low Higgs masses. For this study, all NLO production cross sections are calculated by HIGLU and branching fractions are calculated by HDECAY [2]. These values are summarized in Table I.

In the case of  $h_f$  the gluon-fusion production diagram vanishes and only associated pro-

duction with a W or Z boson and vector boson fusion (VBF) production processes are possible. This results in a reduction in production cross section by about a factor of four; however, this reduction is compensated by the increased diphoton branching fraction in these models, which are enhanced by more than two orders of magnitude.

In the past, there have been phenomenological discussions of searches for  $h_f$  at the Tevatron experiments [3], as well as experimental searches at LEP [4]. In Run I CDF searched for  $h_f$  [5], and in Run II the DØ experiment has published a paper [6] dealing with the  $h_f$  search. Here, the sensitivity of a CDF search for  $h_f$  through the  $h \rightarrow \gamma\gamma$  decay mode will be discussed.

## II. DATA SET, EVENT SELECTION, AND PHOTON ID

This analysis includes data taken between Feb. 2004 and April 2008 and comprises approximately  $3.0 \text{ fb}^{-1}$  of integrated luminosity. Signal Monte Carlo was generated using PYTHIA 6.2 [7] using CTEQ5 [8] parton distribution functions, and the standard CDF UE tune [9].

The diphoton triggers, base event selection, and photon identification requirements are the same as the recently published high-mass search for Randall-Sundrum gravitons decaying to the  $\gamma\gamma$  final state (see Reference [10]) and therefore won't be discussed in detail here. The diphoton triggers and the turn-on were checked with recent CDF data and found to be stable.

Events are required to have at least one reconstructed event vertex and only events which include two central photons with  $|\eta_{det}| < 1.05$  (CC) or one central photon and one plug photon with  $1.2 < \eta_{det} < 2.8$  (CP) are selected. Due to a large  $e^+e^-$  contamination, events with two plug photons are not considered in the analysis. Searches are performed in the CC and CP channels with systematic correlations between channels taken into account. Photon ID efficiencies were studied using electrons from Z boson decays and differences between detector response and CDF simulation of the detector were also corrected based on these studies.

Individual photons are required to have transverse energy greater than  $15 \text{ GeV}$ , while the photon pair is required to have  $M_{\gamma\gamma} > 30 \text{ GeV}/c^2$ . These cuts are designed to ensure that the diphoton triggers are close to 100 % efficient.

These cuts define the base selection which was used for the RS graviton search. For the case of  $h_f$  event selection was studied and optimized in an effort to maximize sensitivity. This model dependent optimization was found to improve the cross section limit by more than a factor of two, and is discussed in Section IV.

### III. THE CDF DETECTOR

The CDF detector is described in many available references [11, 12].

### IV. FERMIPHOBIC PRODUCTION AND OPTIMIZATION

Because  $h_f$  can only be produced via associated production or VBF it is useful to optimize the event selection to take advantage of the extra objects in the event. Since associated production is the dominant process we use it to optimize our selection. The expected number of signal and background events were used to calculate a rough expected limit for each variation of the selection criteria. The expected limit was estimated from a counting experiment based on a  $10 \text{ GeV}/c^2$  mass window for each set of selection criteria.

Cuts in a 4-D grid based on all possible combinations of  $P_T^{\gamma\gamma}$ , or the “or” between cuts on  $P_T^{J2}$ ,  $E_T$ , and  $P_T^{iso}$  were studied. To complete this study a model of the background must be included. The following background scenarios were considered:

1. A background model composed of PYTHIA di-photon MC (25 %), and photon ID sideband events (75 %) to model fake photons. The photon ID sideband is defined by events passing all standard photon ID requirements except that the signal region is excluded by requiring that the Had/Em or isolation requirements fail yet pass a looser version of these cuts.
2. A background model composed of di-photon candidate events outside of the  $10 \text{ GeV}/c^2$  mass window.

In each case the total background was normalized to the total number of signal candidates, then the number passing additional cut requirements was used in the expected limit study.

The 4-D study is hard to visualize, but the result was that a rather high cut on  $P_T^{\gamma\gamma}$  ( $P_T^{\gamma\gamma} > 75 \text{ GeV}/c$ ) is approximately as sensitive as any possible combination of the other cuts. This

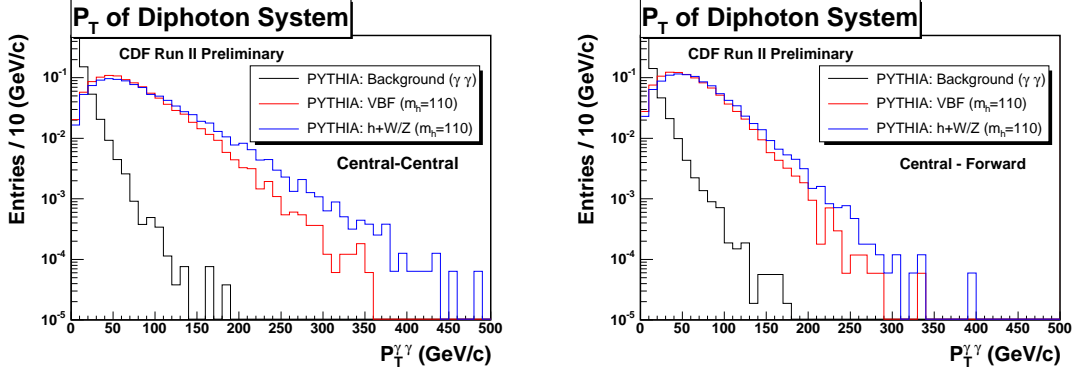


FIG. 1:  $P_T^{\gamma\gamma}$  distributions of the PYTHIA predictions for associated production (blue), VBF (red), and  $\gamma\gamma$  (black) processes for the CC (left) and CP (right) channels.

result was reasonably robust to the choices of background models listed above. Physically, one can imagine that the large  $P_T$  of the  $\gamma\gamma$  pair is equivalent to requiring that something with large transverse momentum balance  $P_T^{\gamma\gamma}$ . That other object can only be jets, leptons, or  $\cancel{E}_T$  so there is not much to gain (other than analysis complication) by making additional requirements to ensure that it was a W or Z boson.

This differs from the standard low mass Higgs searches at CDF because they trigger on leptons or  $\cancel{E}_T$  due to the vector boson, thus removing the option to treat all W/Z final states on an equal footing. The  $P_T$  distributions for the main Higgs production processes and the diphoton background are shown in Figure 1. With this large cut on  $P_T^{\gamma\gamma}$ , roughly 30 % of the associated production signal is maintained while more than 99.5 % of background is removed. Although the cut was optimized based on associated production, VBF also has a very hard  $P_T^{\gamma\gamma}$  spectrum and will be included in the analysis with the same selection. The selection was optimized for the sum of the CC and CP channels.

## V. DETECTOR ACCEPTANCE AND ID EFFICIENCIES

Detector acceptance was studied using PYTHIA Monte Carlo events passed through a parametrized simulation for the CDF detector based on Geant [13] and GFlash [14]. A summary of signal acceptance for each signal process and mass point generated is given in Table II.

Acceptance (%)				
	$h + W/Z$		VBF	
$M_h$	CC	CP	CC	CP
70	2.9	1.8	3.8	2.1
80	3.7	2.4	4.1	2.6
90	4.4	3.1	4.5	3.1
100	5.0	3.8	4.7	3.5
110	5.5	4.5	5.0	3.9
120	6.1	5.2	5.1	4.3
130	6.6	5.7	5.2	4.5
140	7.1	6.3	5.5	4.8
150	7.6	6.9	5.6	5.0

TABLE II: Signal acceptance, in percent, for each signal process and mass point generated after applying the  $P_T^{\gamma\gamma} > 75 \text{ GeV}/c$  cut.

## VI. SYSTEMATIC UNCERTAINTIES

All systematics shown in Table VI are included in this analysis. PDF uncertainty on event acceptance was calculated using the CTEQ61.M [15, 16] error sets and a standard event re-weighting technique [17, 18]. ISR and FSR uncertainties were studied using MC samples with modified parton shower parameters. The energy scale systematic uncertainty of the CEM/PEM was studied by checking the effect on the acceptance of varying the CEM/PEM scale by 1 %. An additional systematic uncertainty on the acceptance was included due to potential higher order effects on the shape of the  $P_T^{\gamma\gamma}$  distribution.

The uncertainty on efficiency from  $\gamma \rightarrow e^+e^-$  conversions is due to the uncertainty on material included in the simulation of the CDF detector. Photon ID efficiencies were studied using electrons from  $Z$  boson decays; however, there are small differences in the shower profiles of electrons and photons which may affect these studies. To account for this, a systematic was taken based on the differences between photon and electron efficiencies observed in the MC with detector simulation. A single data-MC scale factor is applied to the full MC

sample; however, the variations of this factor between data taking periods was included as a systematic. Finally, the uncertainties on the fits used to study ID efficiencies are propagated as an uncertainty.

	Systematic Errors (%)	
	Central - Central	Central - Forward
PDF	2	2
IFSR	4	4
E Scale	2	3
NLO v/s LO	4	4
Luminosity	6	6
Conversions	0.2	3
Photon/Electron ID	1	2.6
Run Dependence	1.5	2.0
Data/MC fits	0.2	0.8

## VII. BACKGROUND MODEL

The width of the  $M_{\gamma\gamma}$  signal peak (shown in Figure 2) is on the order of a few  $GeV/c^2$  and is only limited by detector resolution. This means that we are searching for a very narrow peak on the smooth background distribution composed of both SM di-photon events and events in which one or two jets fake a photon. Modeling of this background combination is possible but non-trivial and is not necessary for dedicated searches for a narrow mass peak. Therefore, rather than model each background component directly this analysis assumes a null hypothesis - after visual confirmation that no obvious peak exists in the data - and simply fits a smooth curve to mass window sidebands. This fit, for each test Higgs mass, serves as the background model for predicting expected sensitivity and for testing against the data for the signal hypotheses.

Fits of the signal region for CC and CP events are shown in Figures 3. A shape systematic is derived based on the uncertainty on the fit (on the order of 20 %) and is included when setting limits.

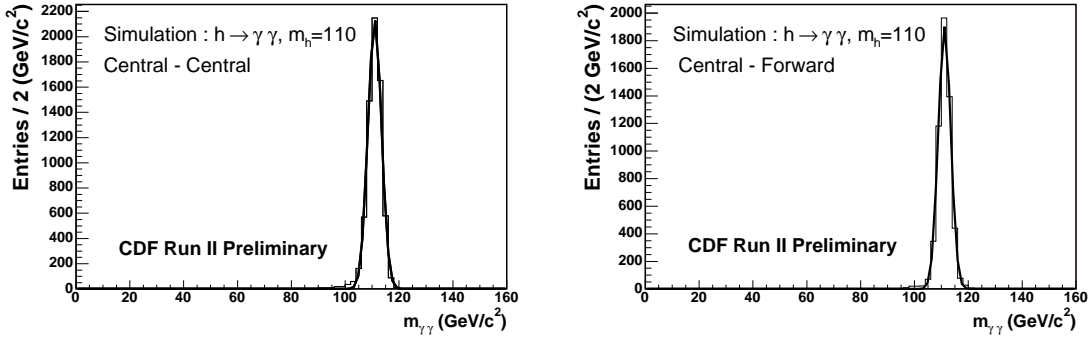


FIG. 2:  $M_{\gamma\gamma}$  mass peak for  $M_h = 110 \text{ GeV}/c^2$  with a Gaussian  $\sigma$  of less than  $3 \text{ GeV}/c^2$ .

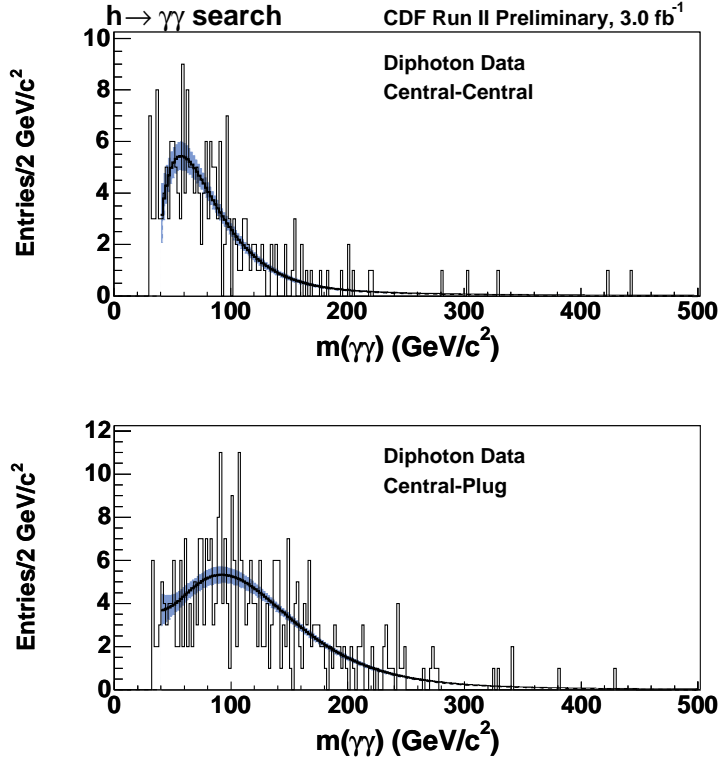


FIG. 3: Smooth fits to the signal region in the CC and CP data with the fermiophobic Higgs event selection. This fit will serve as the null hypothesis background model.

## VIII. RESULTS

The theoretical production cross section, branching fraction, and detector acceptance multiplied by efficiency are given for each mass point in Table I [2] and Table II respectively. These values, as well as the invariant mass distributions for signal and the background model,



will be used to set limits on  $h \rightarrow \gamma\gamma$  production. A binned-likelihood method is applied using Poisson fluctuations of the  $M_{\gamma\gamma}$  bin contents in order to set limits on sensitivity to the  $h \rightarrow \gamma\gamma$  signal hypothesis. The 95 % confidence level limits on cross section multiplied by branching fraction are summarized in Table III. These limits, as well as the limits on the branching fraction, are shown in Figures 4.

$M_h$ ( $GeV/c^2$ )	Expected limit (fb)	+1 $\sigma$ (fb)	-1 $\sigma$ (fb)	Observed limit(fb)
70	88.0	125.9	62.0	68.2
80	68.2	96.4	49.8	95.3
90	57.5	80.2	40.4	87.7
100	48.2	69.5	34.9	44.5
110	41.8	59.2	29.9	46.1
120	36.3	51.0	26.3	30.1
130	27.8	37.9	20.0	22.5
140	26.5	38.1	18.9	24.4
150	23.5	33.6	17.3	23.9

TABLE III: Expected and observed limits as well as the 1  $\sigma$  bands on the expected limit. These limits are only valid for the Fermiophobic Higgs search.

## IX. CONCLUSIONS

A simple analysis was discussed which searched for  $h \rightarrow \gamma\gamma$  in 3.0  $fb^{-1}$  of CDF data. Unfortunately, no significant excess was observed. A fermiophobic model was considered as a benchmark, and a 95 % confidence level limit was set on the production cross sections and branching fractions. A lower limit on the mass of 106  $GeV/c^2$  was set for the benchmark model. This is the strongest limit so far from a hadron collider and is only slightly below the limit set by LEP of 109.7  $GeV/c^2$  [4]. In addition, above 110  $GeV/c^2$  this result excludes a region of branching fractions that has not been excluded by previous collider studies.

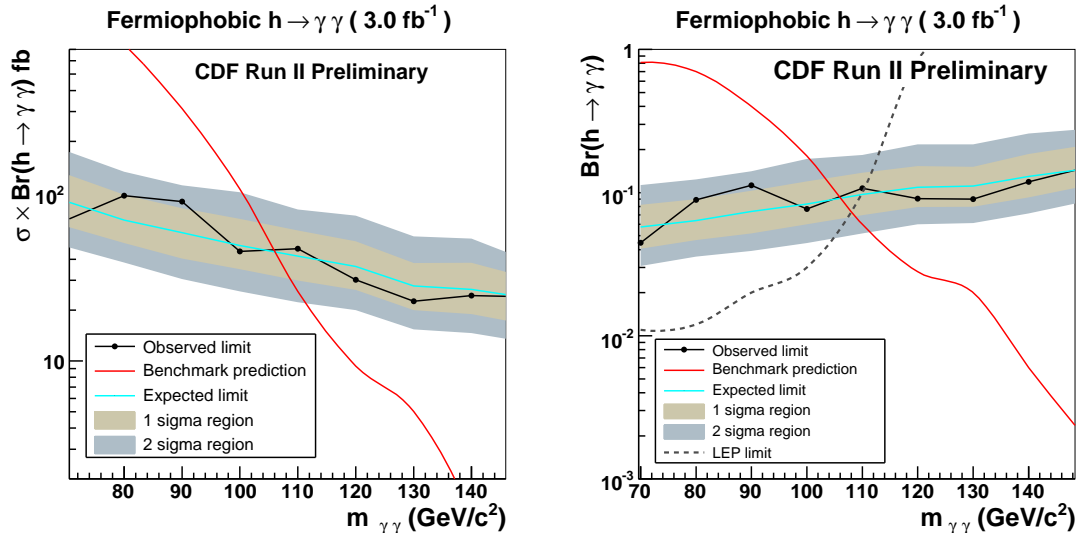


FIG. 4: Cross section times branching fraction limits (left) and branching fraction limits (right) as a function of fermiophobic Higgs mass.

### Acknowledgments

We thank the Fermilab staff and the technical staffs of the participating institutions for their vital contributions. This work was supported by the U.S. Department of Energy and National Science Foundation; the Italian Istituto Nazionale di Fisica Nucleare; the Ministry of Education, Culture, Sports, Science and Technology of Japan; the Natural Sciences and Engineering Research Council of Canada; the National Science Council of the Republic of China; the Swiss National Science Foundation; the A.P. Sloan Foundation; the Bundesministerium für Bildung und Forschung and the Alexander von Humboldt Foundation, Germany; the Korean Science and Engineering Foundation and the Korean Research Foundation; the Science and Technology Facilities Council and the Royal Society, UK; the Institut National de Physique Nucleaire et Physique des Particules/CNRS; the Russian Foundation for Basic Research; the Ministerio de Educación y Ciencia and Programa Consolider-Ingenio 2010, Spain; the Slovak R&D Agency; and the Academy of Finland.

---

[1] S. Mrenna and J. D. Wells, Phys. Rev. **D63**, 015006 (2001), hep-ph/0001226.

[2] M. Spira (1998), hep-ph/9810289.

- [3] G. L. Landsberg and K. T. Matchev, Phys. Rev. **D62**, 035004 (2000), hep-ex/0001007.
- [4] LEP (LEP Higgs Working Group) (2001), hep-ex/0107035.
- [5] A. A. Affolder et al. (CDF), Phys. Rev. **D64**, 092002 (2001), hep-ex/0105066.
- [6] V. Abazov et al. (D0) (2008), arXiv:0803.1514 [hep-ex].
- [7] T. Sjostrand et al., Comput. Phys. Commun. **135**, 238 (2001), hep-ph/0010017.
- [8] H. L. Lai et al. (CTEQ), Eur. Phys. J. **C12**, 375 (2000), hep-ph/9903282.
- [9] R. Field and R. C. Group (CDF) (2005), hep-ph/0510198.
- [10] T. Aaltonen et al. (CDF) (2007), arXiv:0707.2294 [hep-ex].
- [11] F. Abe et al. (CDF), Nucl. Instr. Meth. **A271**, 387 (1988).
- [12] P. T. Lukens (CDF) (2003), fermilab-TM-2198.
- [13] R. Brun, F. Bruyant, M. Maire, A. C. McPherson, and P. Zancarini (1987),  
cern-DD/EE/84-1.
- [14] G. Grindhammer, M. Rudowicz, and S. Peters, Nucl. Instrum. Meth. **A290**, 469 (1990).
- [15] D. Stump et al., JHEP **10**, 046 (2003), hep-ph/0303013.
- [16] J. Pumplin et al., Phys. Rev. **D65**, 014013 (2002), hep-ph/0101032.
- [17] P. M. Nadolsky and Z. Sullivan, eConf **C010630**, P510 (2001), hep-ph/01110378.
- [18] D. Bourilkov, R. C. Group, and M. R. Whalley (2006), hep-ph/0605240.